

## Article

# Recombinant AnAFP Reveals Genetic Contributors to Antifungal Protein Tolerance and Fungal Development in *Aspergillus flavus*

Zunyan Li †, Jiapeng Shi †, Sen Wang, Xueting Huang, Shihua Wang and Yu Wang \*

State Key Laboratory of Agricultural and Forestry Biosecurity, Key Laboratory of Pathogenic Fungi and Mycotoxins of Fujian Province, School of Animal Science, and School of Life Sciences, Fujian Agriculture and Forestry University, Fuzhou 350002, China; 1500315740@qq.com (Z.L.); 2236738618@qq.com (J.S.); 752408220@qq.com (S.W.); 2821735365@qq.com (X.H.); wshyyl@sina.com (S.W.)

\* Corresponding author. E-mail: wangyu@fafu.edu.cn (Y.W.)

† These authors contributed equally to this work.

Received: 5 May 2026; Revised: 21 May 2026; Accepted: 25 June 2026; Available online: 30 June 2026

**ABSTRACT:** *Aspergillus flavus* is an agriculturally important and aflatoxigenic fungus, underscoring the need for alternative antifungal strategies. Cysteine-rich antifungal proteins (AFPs) are promising bioactive molecules, yet their recombinant production and genetic determinants of fungal tolerance remain insufficiently characterized. Here, we investigated AnAFP, an antifungal protein from *Aspergillus niger*, and evaluated its activity against *A. flavus*. Bioinformatic analyses predicted an N-terminal signal peptide, a putative intrinsically disordered region, and a mature cysteine-rich domain structurally related to known fungal AFPs. Guided by these features, the predicted mature region of AnAFP was expressed in *Escherichia coli* and purified through Ni-NTA affinity chromatography, tag cleavage, cation-exchange chromatography, and size-exclusion chromatography. Purified AnAFP inhibited *A. flavus* growth, and comparison with PgAFP and AfAFP confirmed antifungal activity at micromolar concentrations. To identify genes associated with AFP tolerance,  $\Delta adol$ ,  $\Delta defl$ , and  $\Delta adk1$  mutants were generated by homologous recombination. All three mutants showed increased sensitivity to AnAFP, PgAFP, and AfAFP relative to the wild-type strain, suggesting that *adol*, *defl*, and *adk1* may contribute to AFP tolerance. Deletion of these genes also affected colony growth, conidiation, sclerotial formation, stress responses, and aflatoxin production. These findings establish a recombinant production strategy for AnAFP and provide preliminary evidence linking *adol*, *defl*, and *adk1* to AFP sensitivity and fungal physiology more broadly in this pathogenic and aflatoxigenic species.

**Keywords:** *Aspergillus flavus*; AnAFP; Antifungal protein; Aflatoxin B1

## 1. Introduction

*Aspergillus flavus* (*A. flavus*) is a saprophytic filamentous fungus with broad ecological adaptability, commonly colonizing plant debris, animal silage, and deteriorated grain-derived substrates [1], with a particular prevalence in maize, cottonseed, and tree nuts [2]. Beyond its environmental and agricultural



relevance, *A. flavus* is also recognized as an opportunistic human pathogen and has been recovered from tracheal aspirates of patients with COVID-19 [3]. A major public health concern associated with this species is its capacity to biosynthesize aflatoxins, including aflatoxin B<sub>1</sub> (AFB<sub>1</sub>), B<sub>2</sub>, G<sub>1</sub>, G<sub>2</sub>, and related derivatives, among which AFB<sub>1</sub> is regarded as one of the most potent naturally occurring hepatocarcinogens [4]. Conventional strategies to control *A. flavus* contamination have relied largely on fungicides. However, the extensive use of azole-class antifungal agents has contributed to the emergence of isolates with clinically relevant resistance phenotypes. For example, a clinical surveillance study conducted between 2020 and 2023 in central China reported that 18.5% of clinical *A. flavus* isolates exhibited resistance to itraconazole [5]. These observations underscore the urgent need to develop alternative, environmentally compatible strategies to suppress *A. flavus* proliferation and reduce aflatoxin contamination. In this context, antifungal proteins and peptides have attracted increasing attention as promising “green” antifungal agents because of their biodegradability, suitability for fermentative production, and generally low cytotoxicity toward mammalian cells [6].

Antimicrobial proteins and peptides comprise a diverse group of bioactive molecules produced across a wide phylogenetic spectrum, ranging from bacteria to humans. Among them, antifungal proteins, hereafter referred to as AFPs, represent a distinct class of antifungal biomolecules. In filamentous ascomycetes, AFPs are predominantly produced by species belonging to *Aspergillus*, *Penicillium*, *Neosartorya*, and related genera [7]. Representative examples include the antifungal protein AFP from *Aspergillus giganteus* [8], the *Penicillium chrysogenum* antifungal protein PAF [8], and the anti-yeast protein NFAP2 from *Neosartorya fischeri* [9]. These proteins generally exhibit potent antifungal activity against agriculturally important phytopathogens, including *Fusarium graminearum* and *Botrytis cinerea* [10,11]. AFPs have been isolated from native fungal cultures; however, this approach is frequently constrained by low production yields, labor-intensive purification procedures, and limited scalability [12]. Recent work from our group has demonstrated that codon optimization and fusion with solubility-enhancing partners, such as thioredoxin (Trx), can substantially improve the recombinant production of AFPs in *Escherichia coli* (*E. coli*) [13]. Nevertheless, whether this strategy can be broadly applied to other AFPs or structurally related antifungal proteins remains to be further validated through experimental investigation.

Small cysteine-rich antifungal proteins have been recognized for several decades; nevertheless, their precise mechanisms of action remain incompletely understood. Current evidence indicates that these proteins exert antifungal activity through multiple cellular processes. One major mechanism involves disruption of fungal cell wall integrity, partly through inhibition of chitin synthase activity in susceptible fungi, including *Aspergillus niger* (*A. niger*), *Aspergillus oryzae*, and *Fusarium oxysporum* [14–17]. In addition, some AFPs can compromise plasma membrane integrity by inducing pore formation and potassium efflux, whereas PAF has been reported to promote membrane hyperpolarization followed by calcium influx [18]. Beyond cell wall disruption and membrane perturbation, AFPs can also interfere with key intracellular signaling networks. For example, the *Penicillium chrysogenum* antifungal protein PAF has been shown to activate heterotrimeric G-protein signaling and modulate downstream PKC/MPK and cAMP/PKA pathways in sensitive fungal cells [19]. Recently, our group identified Npt1 as a previously uncharacterized protein that regulates AFP activity, further suggesting that the antifungal effects of AFPs may involve additional molecular determinants [13]. In this study, we focus on AnAFP, a cysteine-rich antifungal protein originally isolated from *A. niger* [20]. AnAFP is of particular interest because its antifungal spectrum, feasibility for recombinant production, and mechanistic basis remain insufficiently characterized. Moreover, whether our previously established expression strategy can be effectively applied to AnAFP requires further investigation.

The fully sequenced *A. niger* genome and available transcriptomic and proteomic datasets for the reference strain CBS 513.88 [21] provide useful resources for studying AnAFP activity and its potential molecular mechanisms. Genetic screening of the plant defensin HsAFP1 in *Saccharomyces cerevisiae*

identified 13 resistant mutants and 71 hypersensitive mutants, many of which carried mutations in genes associated with mitochondrial function [22]. Notably, *ado1*, a gene essential for S-adenosylmethionine (SAM) biosynthesis, was identified as a key determinant of HsAFP1 resistance [23]. In addition, *def1*, which encodes a nuclear RNA polymerase II degradation factor, and *adk1*, which encodes adenylate kinase involved in adenine nucleotide homeostasis, ATP metabolism, and DNA replication, have been shown to modulate cellular sensitivity to HsAFP1 [22,24]. These findings suggest that susceptibility to antifungal proteins is closely associated with mitochondrial function, nucleotide metabolism, and broader cellular energy-homeostasis pathways in fungi. However, the roles of the corresponding *ado1*, *def1*, and *adk1* homologs in the pathogenic and aflatoxigenic fungus *A. flavus*, particularly in relation to AnAFP sensitivity, remain to be elucidated. Investigating these homologs may provide new mechanistic insights into how AnAFP affects pathogenic fungal physiology and may help identify conserved determinants of susceptibility to cysteine-rich antifungal proteins.

In this study, we expressed and purified the recombinant antifungal proteins AnAFP, PgAFP, and AfAFP in *E. coli* and confirmed their inhibitory activities against *A. flavus*. To elucidate the molecular determinants underlying their antifungal effects, we generated *A. flavus* deletion mutants of *ado1*, *def1*, and *adk1* using homologous recombination and examined their sensitivities to each AFP. These findings provide a foundation for further studies on the antifungal activity and potential mechanisms of AFPs in *A. flavus*.

## 2. Methods

### 2.1. Strains and Culture Conditions

The *E. coli* strains *DH5 $\alpha$*  and *BL21* were used for plasmid DNA preparation and recombinant protein expression, respectively. In this study, the wild-type *A. flavus* (WT) strain ( $\Delta ku70$ ) was maintained in our laboratory. The *CA14PTs* strain ( $\Delta ku70$ ;  $\Delta pyrG$ ), used to construct other mutant strains, was kindly provided by Dr. Perng-Kuang Chang [25]. The growth of the *A. flavus* strains was evaluated on YGT media (comprising 6 g/L yeast extract, 20 g/L glucose, 1 mL/L trace elements, and 1.5% agar) at 37 °C or 28 °C. Sclerotia production of the strains was assessed on CM media (complete medium containing 6 g/L yeast extract, 6 g/L peptone, 10 g/L sucrose, and 1.5% agar), and aflatoxin biosynthesis was examined in a YES liquid culture (yeast extract/sucrose medium; 2% yeast extract, 150 g/L sucrose, and 1 g/L MgSO<sub>4</sub>·7H<sub>2</sub>O) at 28 °C. The trace element solution (100 mL) consisted of 2.2 g of ZnSO<sub>4</sub>·7H<sub>2</sub>O, 1.1 g of H<sub>3</sub>BO<sub>3</sub>, 0.5 g of MnCl<sub>2</sub>·4H<sub>2</sub>O, 0.5 g of FeSO<sub>4</sub>·7H<sub>2</sub>O, 0.17 g of CoCl<sub>2</sub>·5H<sub>2</sub>O, 0.16 g of CuSO<sub>4</sub>·5H<sub>2</sub>O, 0.005 g of (NH<sub>4</sub>)<sub>6</sub>Mo<sub>7</sub>O<sub>24</sub>·5H<sub>2</sub>O, and 4.45 g of Na<sub>2</sub>EDTA.

### 2.2. Mutant Strain Construction

The *A. flavus* strain referred to as WT in this study was the  $\Delta ku70$  strain maintained in our laboratory. The *CA14PTs* strain, a  $\Delta ku70$ ;  $\Delta pyrG$  derivative, was used as the recipient strain for targeted gene deletion because the  $\Delta pyrG$  background enables selection with the *A. fumigatus pyrG* marker. The  $\Delta ado1$ ,  $\Delta def1$ , and  $\Delta adk1$  mutants were generated in the *CA14PTs*/ $\Delta ku70$  background by homologous recombination and were compared with the  $\Delta ku70$  WT strain in subsequent phenotypic analyses. A homologous recombination strategy was used to generate a deficient strain. In brief, the upstream and downstream flanking regions of the target gene and the *A. fumigatus pyrG* nutritional marker were amplified using specific primers. The fragments were then purified using a gel extraction kit and subsequently fused using overlap extension PCR to construct a homologous recombination cassette. The final fusion PCR product was further purified and transformed into *CA14PTs* strain protoplasts. The protoplasts were prepared by digesting the cell wall of freshly collected mycelium using an enzymatic solution containing 20 mM NaH<sub>2</sub>PO<sub>4</sub> (pH 5.8), 20 mM CaCl<sub>2</sub>, 1.2 M NaCl, Snailase (7.5 g/mL), lysozyme (7.5 g/mL), lywallzyme (7.5 g/mL), and 3 mg/mL driselase. The mixture was incubated at 29 °C with shaking at 180 rpm for 1–1.5 h. The efficiency of the

enzymatic lysis of the mycelium's cell wall was assessed under a microscope after 1 h. The truncated mutation strains of *ado1*, *def1*, and *adk1* were all generated in this manner. Putative positive transformants were validated using diagnostic PCR [26].

### 2.3. Protein Expression and Purification

In this study, we chose the mature form of AnAFP to express in the *E. coli* system. The gene encoding AnAFP was produced by using full gene synthesis with codon optimization and subsequently cloned into a pET-32a expression vector. The resulting constructs included a 6×His-tag and a Trx-tag at the N-terminus, followed by a PreScission protease recognition site before the target protein. After verification, the plasmids were individually transformed into *BL21*. The transformed cells were propagated in 10 mL of LB medium supplemented with 100 µg/mL ampicillin, and incubated at 37 °C with 180 rpm agitation for 12 h. Subsequently, cultures expressing either AnAFP were scaled up to 4 L of fresh LB medium with 100 µg/mL ampicillin and maintained under identical conditions until the optical density at 600 nm reached 0.5. Cells were then collected, resuspended in pre-cooled lysis buffer (comprising 50 mM Tris-HCl, 500 mM NaCl, and 20 mM imidazole, adjusted to pH 7.4), and disrupted by sonication on ice. The lysates were clarified by centrifugation at 12,000× g for 20 min at 4 °C for three times, and the supernatant was then applied to a Ni-NTA affinity column. A stepwise elution was performed using buffers with increasing concentrations of imidazole (from 20 to 300 mM) to selectively bind and subsequently elute the His-tagged fusion protein. The fusion tag was cleaved by incubating the protein with PreScission protease 3C at 4 °C for 16 h, followed by post-dialysis of the eluted fractions against a buffer composed of 50 mM Tris-HCl and 10 mM NaCl. The proteolytic reaction mixture was further subjected to ion-exchange chromatography using a Cytiva S cation exchange chromatography column. A linear gradient of NaCl was used for elution in an ÄKTA pure™ chromatography system, which yielded highly purified AnAFP. Size-exclusion chromatography was performed for the final purification using a Superdex 75 10/300 GL column, which was equilibrated and eluted with a buffer of 50 mM Tris-HCl and 150 mM NaCl. The recombinant protein AnAFP was resolved by electrophoresis [26].

### 2.4. Analysis of Antifungal Activity of AFPs

Each 1.5-mL Eppendorf tube was filled with 1 mL of YGT liquid medium. Gradient concentrations of PgAFP, AfAFP, and AnAFP proteins were added to the medium. The MIC was defined as the lowest protein concentration required to completely inhibit macroscopic fungal growth. To achieve a final spore concentration of  $1 \times 10^4$  spores/mL, 1 µL of a spore suspension containing  $1 \times 10^7$  spores/mL was introduced into each tube. The fungal strains *ado1*, *def1*, *adk1*, or the WT strain were incubated at 37 °C with continuous shaking at 180 rpm for 48 h [27].

### 2.5. Quantitative Reverse Transcription-Polymerase Chain Reaction Assay

RT-qPCR was performed as previously described, with minor modifications. [28,29]. To remove possible residual genomic DNA (gDNA), the total RNA (5 µg) was first treated with DNase I (Thermo Fisher Scientific, Waltham, MA, USA), gDNA free RNA (1 µg) was reverse-transcribed into cDNA by using the HRbioTMIII Aid First-strand cDNA Synthesis kit (Heruibio, Fuzhou, China). Finally, the quantitative reverse transcription-polymerase chain reaction (RT-qPCR) was performed with the SYBR Green Premix kit (Takara, Dalian, China), and the instrument M×3000p thermocycler (Agilent Technologies, Santa Clara, CA, USA). The  $2^{-\Delta\Delta Ct}$  method was applied to evaluate the expression levels of corresponding target genes. The primers of the RT-qPCR assay are listed in Table S1. The  $\beta$ -actin gene was selected as the reference gene.

## 2.6. Analysis of Vegetative Growth and Sclerotia Formation

The colony diameter was evaluated using YG solid media plates inoculated with a spore suspension at a concentration of  $10^7$  spores/mL. The plates were then incubated at 37 °C for 4 days in the dark. Post-incubation, photographs were obtained to document the colony morphology, and the colony diameters were measured. Conidia production was compared using YGT solid media plates similarly inoculated with  $10^7$  spores/mL and incubated at 37 °C for 4 days in the dark. Following incubation, the plates were washed with sterile water to collect the spores. Conidial count was determined using a hemocytometer. Sclerotia production was analyzed using fresh spore suspensions of both mutant and WT strains at  $10^7$  spores/mL inoculated onto CM solid medium plate, and incubated in the dark at 37 °C for 7 days. The aerial mycelium and conidia were removed by washing with 75% ethanol, and the plates were photographed. The sclerotia morphology was captured using a stereomicroscope, and the sclerotia were quantified from the magnified images based on a quarter section of the colony [30].

## 2.7. Thin-Layer Chromatography Analysis

To extract aflatoxin from the cultured liquid medium, fresh spore suspensions of various *A. flavus* strains, including WT strain and gene-edited strains, at a concentration of  $10^7$  spores/mL were inoculated into 10 mL of YES liquid medium. The cultures were incubated in the dark at 29 °C for 5 days. Subsequently, 7 mL of the post-cultivation medium was collected, and an equivalent volume of dichloromethane was added to each sample. After thorough mixing, the resulting mixture was shaken at 180 rpm for 30 min and then immediately centrifuged. A 5 mL aliquot of the dichloromethane layer (the lower layer) was extracted for subsequent analysis. For the analysis, 10 µL of each dissolved sample was applied to silica gel plates. A developing solvent with a dichloromethane to acetone ratio of 9:1 was used. Plates were imaged under UV illumination using identical exposure settings within each experiment. AFB<sub>1</sub> band intensity was quantified by densitometric analysis using GeneTools software (version 4.3.9). The integrated density of each AFB<sub>1</sub> band was measured, and the local background signal was subtracted from the same lane. The background-corrected intensity of each sample was normalized to the corresponding WT control on the same TLC plate, which was set as 1.0. Data were calculated from three independent biological replicates and are presented as mean ± SD [31].

## 2.8. Pathogenicity Analysis

A pathogenicity analysis of deletion strains on peanut and maize seeds was conducted following the method. To prevent germination, embryos were removed from both types of seeds. Uniformly sized seeds were selected and sterilized by washing with 0.5% sodium hypochlorite for 3 min, followed by rinsing with sterile water to remove any sodium hypochlorite residue. Subsequently, the seeds were soaked in 75% ethanol for 15 s, washed several times with sterile water, and soaked in sterile water for 5 min to completely remove the ethanol. The sterilized seeds were then placed on sterilized filter paper to remove excess water. For testing the pathogenicity of the deletion strains, sterilized peanut or maize seeds were immersed in a spore suspension with  $10^3$  spores/mL for 30 min. Filter paper was placed on Petri dishes, 1 mL of sterile water was added, and the seeds were placed on the filter paper. The seeds were incubated at 29 °C in the dark for 7 days. For the spore count analysis, 20 mL of sterile water was added to the cultured seeds, and the spore suspension was diluted before counting using a hemocytometer. For metabolite extraction, dichloromethane was added to the spore suspension at a 1:1 ratio. The resulting mixture was incubated at 37 °C with continuous shaking at 180 rpm for 10 min, Thin-layer chromatography analysis of aflatoxins was conducted following the method described above [32].

## 2.9. Statistical Analysis and Reproducibility

The samples were chosen through a random selection process to ensure an unbiased and representative dataset. Data analysis was conducted using GraphPad Prism 10.0 and OriginPro 2023, and statistical significance was assessed by means of one-way ANOVA. Differences were considered statistically significant as \*  $p < 0.05$ , \*\*  $p < 0.01$ , and \*\*\*  $p < 0.001$ . All analyzes were performed on a minimum of three biological replicates unless otherwise specified.

## 3. Results

### 3.1. Bioinformatic Characterization of AnAFP

As noted in the introduction, the nomenclature of AFPs has expanded with the continued discovery of new family members [33,34]. To further investigate AFP-mediated inhibition of fungal growth, we analyzed an AFP from *A. niger*, hereafter referred to as AnAFP. Protein sequence information and structural annotation of AnAFP were obtained from the UniProt database. AnAFP was identified from *A. niger* through sequence alignment (Figure 1A). ProtScale analysis indicated that hydrophilic regions, characterized by negative GRAVY values, were more prominent than hydrophobic regions (Figure 1B). SignalP 6.0 predicted a Sec/SPI signal peptide at residues 1–18, with a cleavage site between residues 18 and 19 (Figure 1C). Accordingly, the signal peptide was excluded from the recombinant expression construct. Consistent with this prediction, UniProt analysis showed low confidence scores across residues 1–36 (Figure 1D), suggesting that this region may be intrinsically disordered [35]. Because intrinsically disordered regions often mediate weak, context-dependent interactions and may affect recombinant expression, this N-terminal segment was removed for expression in *E. coli*. Homology modeling using SWISS-MODEL predicted that AnAFP adopts a tertiary structure similar to that of PeAFPB (Figure 1E), and this structural similarity was further supported by alignment using RCSB PDB tools (Figure 1F). Together, these bioinformatic analyses suggest that AnAFP shares structural features with known AFPs and may possess antifungal activity.

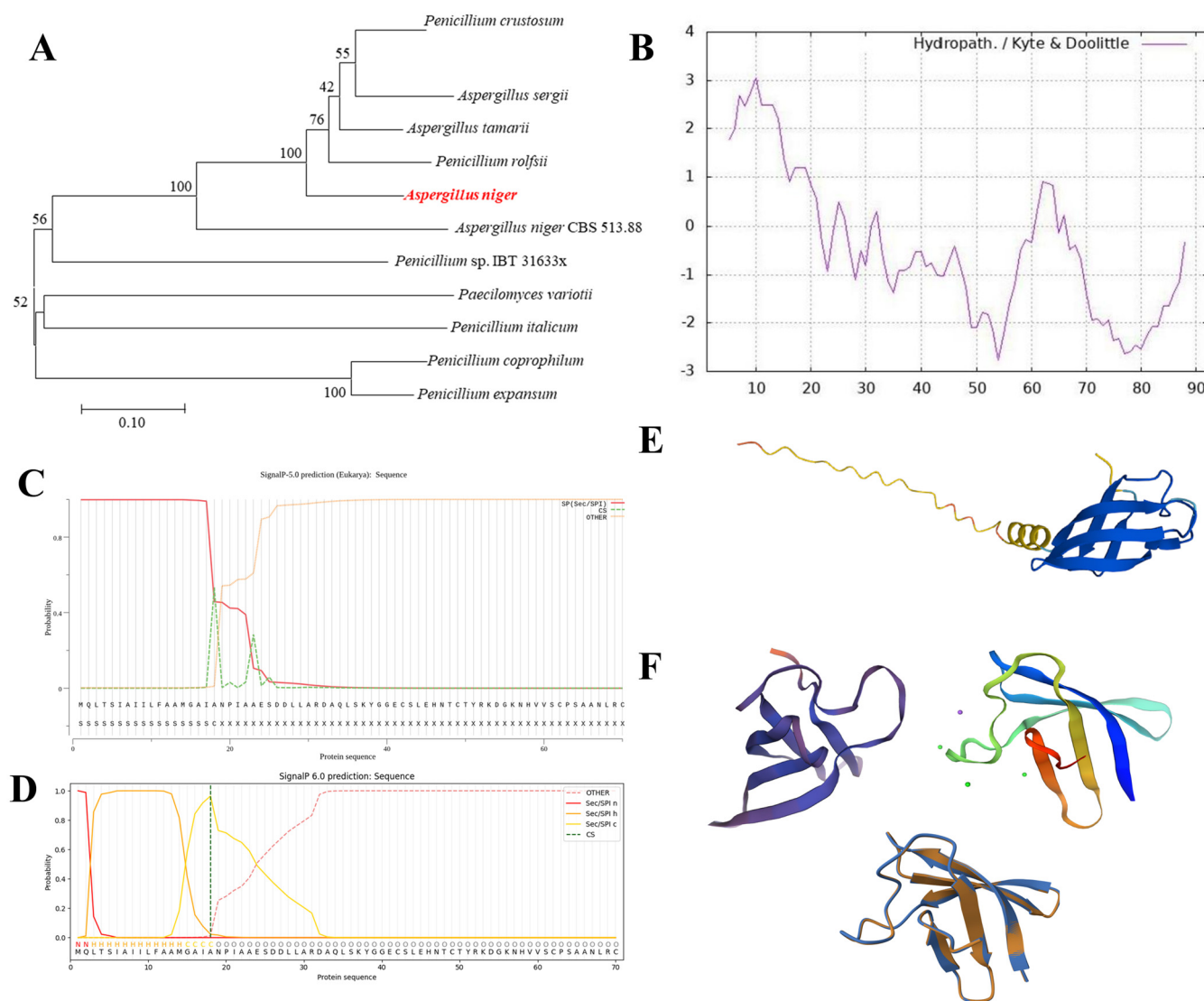


**Figure 1.** Bioinformatic characterization of AnAFP. (A) Sequence-based identification of AnAFP from *Aspergillus niger* by phylogenetic analysis. (B) The hydropathy profile of AnAFP was predicted using the Kyte-Doolittle method, indicating the hydrophilic nature of the protein. (C) SignalP 6.0 prediction of the N-terminal signal peptide and putative cleavage site of AnAFP. (D) Predicted architecture of AnAFP showing the signal peptide, putative propeptide, predicted intrinsically disordered region, and mature peptide. (E) Predicted three-dimensional structure of AnAFP generated by homology modeling. (F) Structural superposition of AnAFP with the homologous antifungal protein PeAFPB.

### 3.2. Expression and Purification of AnAFP and Its Inhibitory Activity Against *A. flavus*

The coding sequence of AnAFP was obtained by whole-gene synthesis and subsequently inserted into the pET-32a expression vector to generate the pET-32a-AnAFP construct (Figure 2A). Recombinant clones were verified by PCR using T7 promoter and T7 terminator primers, and the correct insert was further confirmed by Sanger sequencing. After confirmation, small-scale expression was performed to confirm the production of Trx-6×His-AnAFP (Figure 2B). The recombinant fusion protein was then purified by Ni-NTA affinity chromatography (Figure 2C). The Trx-6His fusion tag was then removed as shown in Figure 2C, and the target protein was further purified by cation-exchange chromatography using a Cytiva cation-exchange column. In a low-salt buffer containing 50 mM Tris-HCl and 10 mM NaCl at pH 7.4, the basic properties of AnAFP allowed selective binding to the cation-exchange column, whereas most contaminating proteins were removed (Figure 2D). SDS-PAGE analysis showed that the resulting protein preparation had relatively high purity (Figure 2E). The purity and homogeneity of AnAFP were further

assessed by size-exclusion chromatography (Figure 2F), confirming a purified protein preparation (Figure 2G). PgAFP and AfAFP were purified according to a previously described method [13]. In vitro antifungal assays using concentration gradients showed that all three purified antifungal proteins, AnAFP, PgAFP, and AfAFP, inhibited the macroscopic growth of *A. flavus* under the tested purified-protein assay conditions. Based on the macroscopic growth endpoint after 48 h of incubation, the MIC values for AnAFP, PgAFP, and AfAFP were determined to be 16, 8, and 4  $\mu\text{M}$ , respectively. Representative cultures at these concentrations are shown in Figure 2H.

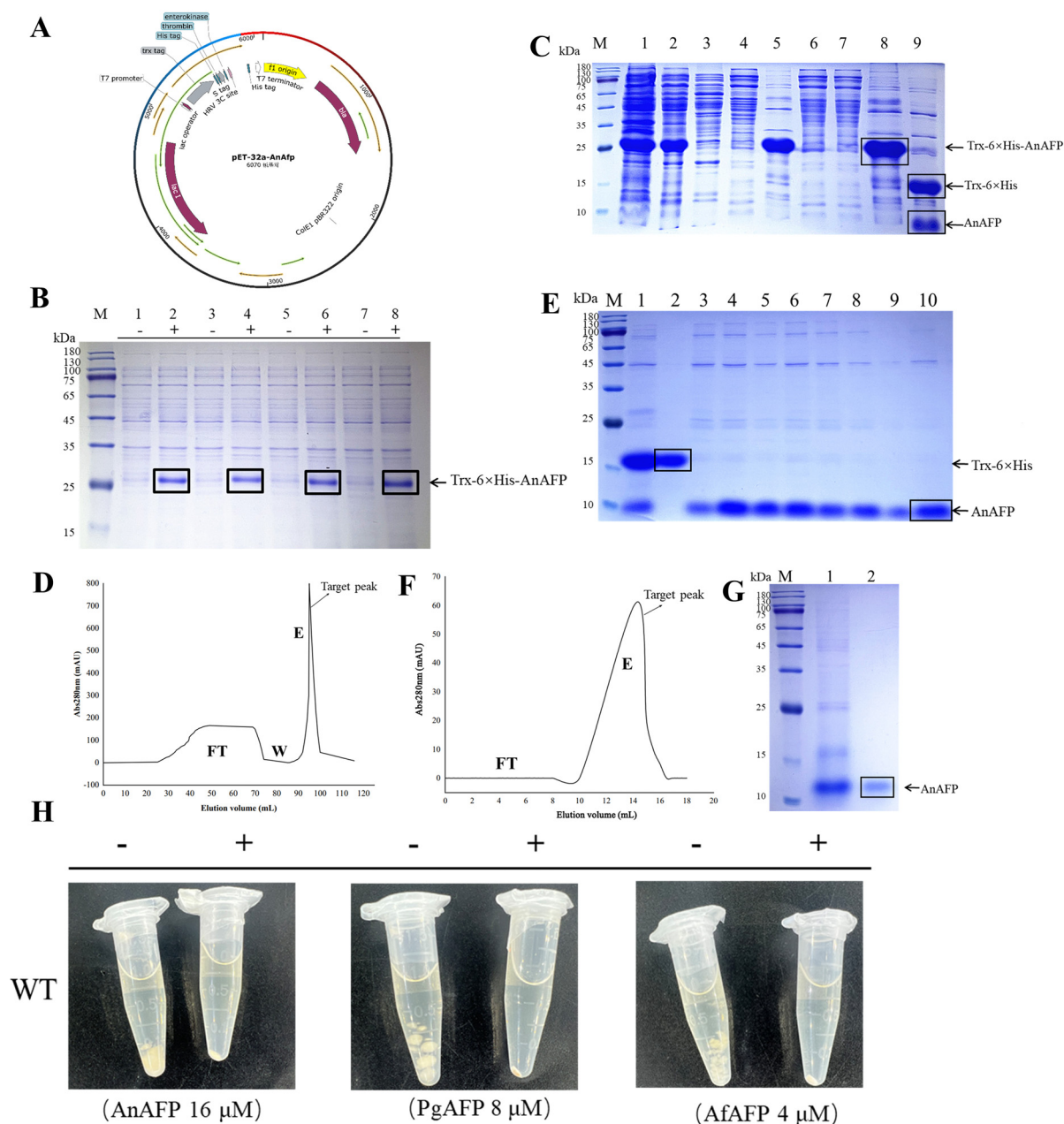


**Figure 2.** Recombinant production, purification, and antifungal activity of AnAFP. (A) Schematic representation of the pET-32a-AnAFP expression construct, showing the T7 promoter, Trx tag, 6 $\times$ His tag, protease cleavage site, and inserted AnAFP fragment. (B) SDS-PAGE analysis of small-scale expression of Trx-6 $\times$ His-AnAFP. (C) SDS-PAGE analysis of Trx-6 $\times$ His-AnAFP purified by Ni-NTA affinity chromatography. (D) Cation-exchange chromatography profile of AnAFP purification using a Cytiva S column. FT, flow-through; W, wash; E, elution. (E) SDS-PAGE analysis of AnAFP-containing fractions obtained from cation-exchange chromatography. Black boxes indicate the target protein bands. (F) Size-exclusion chromatography profile of purified AnAFP. (G) SDS-PAGE analysis of the final purified AnAFP preparation. Black boxes indicate the target protein bands. (H) Representative antifungal assay showing the inhibitory effect of purified AnAFP against *A. flavus*.

### 3.3. *ado1*, *def1*, and *adk1* Affect the Sensitivity of *A. flavus* to AFPs

Previous studies have shown that the fungal genes *ado1*, *def1*, and *adk1* are involved in resistance to the *Heuchera sanguinea*-derived antifungal protein HsAFP1 [22]. To determine whether these genes also contribute to the response of *A. flavus* to AFPs, the  $\Delta$ *ado1*,  $\Delta$ *def1*, and  $\Delta$ *adk1* deletion strains were constructed by homologous recombination. The WT strain and three deletion mutants were then treated with AnAFP, PgAFP, and AfAFP, respectively. Compared with the WT strain, the  $\Delta$ *ado1*,  $\Delta$ *def1*, and  $\Delta$ *adk1* mutants showed increased sensitivity to all three AFPs (Figure 3A). To further examine the response of *A. flavus* to AnAFP, the transcript levels of three regulatory genes, *laeA*, *veA*, and *wetA*, were analyzed. *laeA* and *veA* are key regulators involved in fungal secondary metabolism and development [36,37], whereas *wetA* plays an important role in conidial maturation and spore integrity [38]. Following AnAFP treatment, *laeA* expression exhibited distinct response patterns between the WT and mutant strains. Compared with the corresponding untreated controls, *laeA* expression was markedly downregulated in the WT and  $\Delta$ *ado1* strains but was induced in the  $\Delta$ *adk1* mutant (Figure 3B). The *veA* expression was significantly reduced in the WT strain and  $\Delta$ *adk1* strains (Figure 3C). A *wetA* expression was strongly downregulated in the WT strain and  $\Delta$ *def1* strains, whereas it was upregulated in the  $\Delta$ *adk1* mutant (Figure 3D). Because AnAFP treatment and deletion of *ado1*, *def1*, and *adk1* affected fungal development and secondary metabolism-related phenotypes, we selected *laeA*, *veA*, and *wetA* as representative regulatory genes associated with these processes. These results suggest that *ado1*, *def1*, and *adk1* influence AFP sensitivity in *A. flavus* and that their deletion alters AnAFP-induced transcriptional responses of genes associated with fungal development and secondary metabolism.

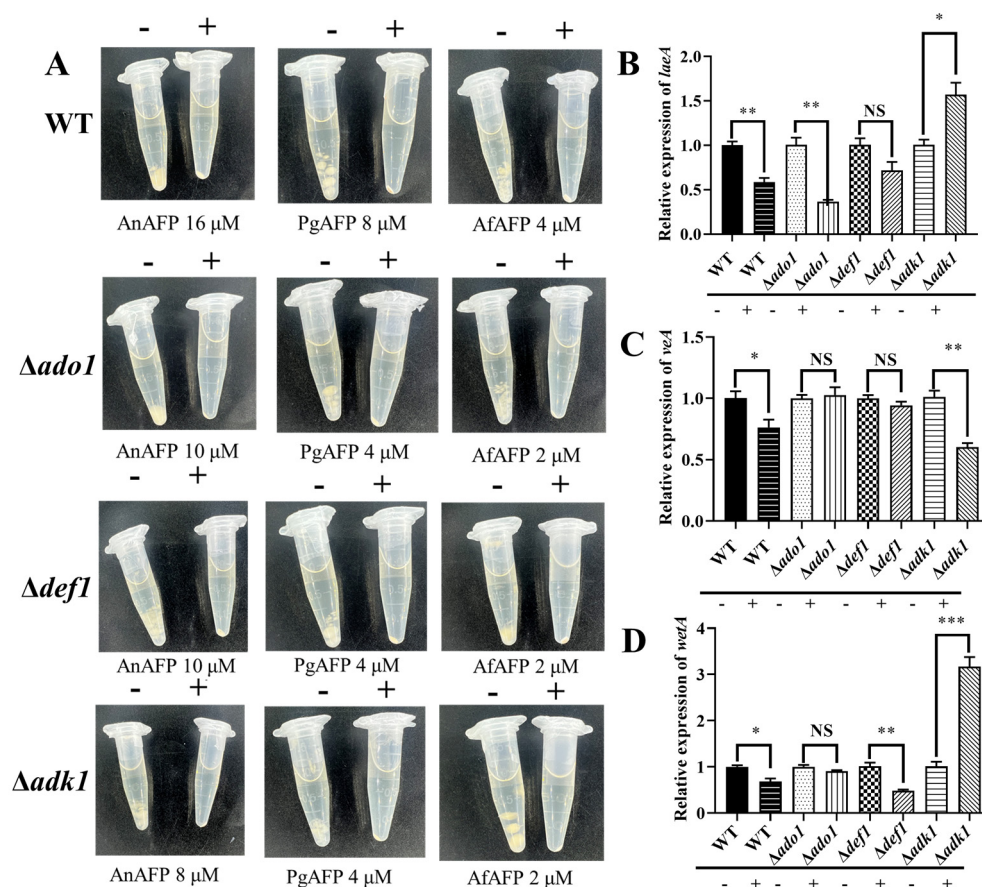


**Figure 3.** Deletion of *ado1*, *def1*, and *adk1* increases AFP sensitivity and alters AnAFP-associated transcriptional responses in *A. flavus*. (A) Antifungal sensitivity assay of the WT strain and  $\Delta$ *ado1*,  $\Delta$ *def1*, and  $\Delta$ *adk1* mutants treated with AnAFP, PgAFP, and AfAFP. The deletion mutants displayed increased sensitivity to the three antifungal proteins compared with the WT strain.

(B–D) Relative expression levels of *laeA* (B), *veA* (C), and *wetA* (D) in the wild-type and mutant strains following AnAFP treatment, as determined by RT-qPCR.  $\beta$ -actin was used as the internal reference gene. Data are presented as the mean  $\pm$  SD from three independent biological replicates. Statistical significance was determined by one-way ANOVA. Differences were considered statistically significant as \*  $p < 0.05$ , \*\*  $p < 0.01$ , and \*\*\*  $p < 0.001$ .

### 3.4. Deletion of *ado1*, *def1*, and *adk1* Affects Fungal Development and Aflatoxin Production in *A. flavus*

Deletion of *ado1*, *def1*, and *adk1* markedly affected the growth and development of *A. flavus*. Compared with the WT strain, the  $\Delta$ *ado1*,  $\Delta$ *def1*, and  $\Delta$ *adk1* mutants all exhibited reduced colony diameters (Figure 4A), with the most pronounced reductions observed in the  $\Delta$ *ado1* and  $\Delta$ *def1* strains (Figure 4B). On YGT medium, colonies of the  $\Delta$ *adk1* strain appeared completely white (Figure 4A), suggesting altered pigment production. Microscopic observation showed that all three deletion mutants formed smaller conidial heads and displayed a sparser distribution of conidiophores than the WT strain (Figure 4C). Consistently, spore quantification revealed that all three mutants produced markedly fewer spores than the WT strain (Figure 4D). Sclerotial development was also affected by the deletion of these genes. In the  $\Delta$ *ado1* strain, sclerotia were more concentrated near the center of the culture plate (Figure 4E), although the total number of sclerotia was comparable to that of the WT strain (Figure 4F). In contrast, the  $\Delta$ *def1* and  $\Delta$ *adk1* strains produced substantially fewer sclerotia than the WT strain (Figure 4F), suggesting that *def1* and *adk1* contribute to sclerotial formation in *A. flavus*. Aflatoxin production was further examined by thin-layer chromatography (TLC) (Figure 4G). Quantification of TLC band intensity showed that the  $\Delta$ *ado1* and  $\Delta$ *adk1* strains accumulated lower levels of aflatoxin than the WT strain (Figure 4H,J), whereas the  $\Delta$ *def1* strain showed increased aflatoxin production (Figure 4I).

To assess whether *ado1*, *def1*, and *adk1* influence the expression of developmental and secondary metabolism-related regulators, we quantified the transcript levels of *laeA*, *veA*, and *wetA* by RT-qPCR. Under normal growth conditions without AnAFP treatment, *laeA* was upregulated in  $\Delta$ *ado1* relative to the WT strain, whereas *veA* was downregulated in  $\Delta$ *def1*. In  $\Delta$ *adk1*, both *laeA* and *wetA* showed lower basal expression levels than those in the WT strain (Figure 4K).

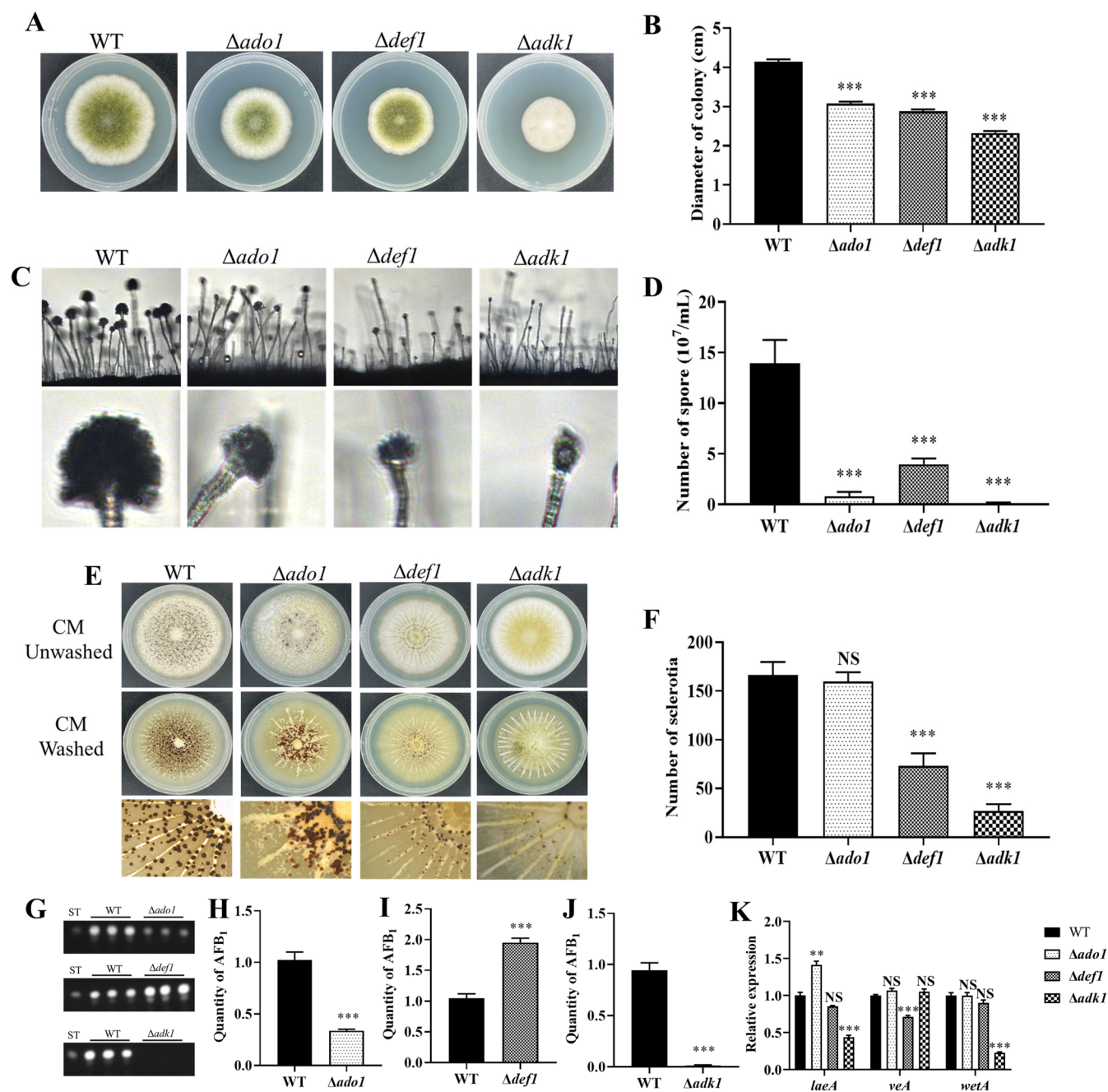


**Figure 4.** Effects of *ado1*, *def1*, and *adk1* deletion on vegetative growth, conidiation, sclerotial formation, and aflatoxin production in *A. flavus*. (A) Colony morphology of the WT strain and  $\Delta ado1$ ,  $\Delta def1$ , and  $\Delta adk1$  mutants grown on YGT medium. (B) Quantification of colony diameter. (C) Microscopic observation of conidiophores and conidial heads in the WT strain and mutant strains. (D) Quantification of conidia production. (E) Sclerotial formation of the wild-type and mutant strains grown on CM medium under dark conditions. (F) Quantification of sclerotia production. (G) Thin-layer chromatography (TCL) analysis of aflatoxin production in the WT strain and mutant strains cultured in YES medium. (H–J) Quantitative analysis of aflatoxin production in  $\Delta ado1$  (H),  $\Delta def1$  (I), and  $\Delta adk1$  (J) relative to the wild-type strain. (K) Relative expression levels of *laeA*, *veA*, and *wetA* in  $\Delta ado1$ ,  $\Delta def1$ , and  $\Delta adk1$  compared with the WT strain, as determined by RT-qPCR.  $\beta$ -actin was used as the internal reference gene. Data are presented as the mean  $\pm$  SD from three independent biological replicates. Statistical significance was determined by one-way ANOVA. Differences were considered statistically significant at \*\*  $p < 0.01$  and \*\*\*  $p < 0.001$ .

### 3.5. Deletion of *ado1*, *def1*, and *adk1* Alters Stress Responses in *A. flavus*

Given the close association between fungal development, secondary metabolism, and stress adaptation, we further assessed the responses of the three deletion mutants to different stress conditions. Under SDS-

induced plasma membrane stress, all three mutants exhibited higher growth inhibition rates than the WT strain, indicating increased sensitivity to membrane perturbation (Figure 5A). Under CFW-induced cell wall stress, the  $\Delta adol$  mutant displayed an approximately threefold lower growth inhibition rate than the WT strain (Figure 5A). Under  $H_2O_2$ -induced oxidative stress, the  $\Delta adol$  and  $\Delta defl$  mutants showed reduced growth inhibition relative to the WT strain, whereas the  $\Delta adk1$  mutant showed a response comparable to that of the WT strain under the same condition (Figure 5B). Together, these results suggest that *adol*, *defl*, and *adk1* differentially affect colony growth, conidiation, sclerotial development, aflatoxin production, and stress in *A. flavus*.

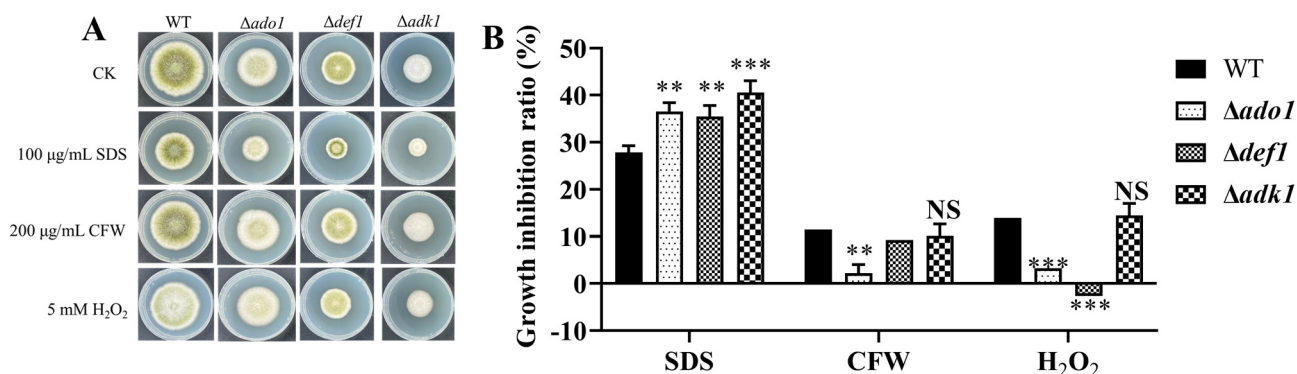


**Figure 5.** Deletion of *adol*, *defl*, and *adk1* alters stress responses in *A. flavus*. (A) The strains were grown on YGT medium supplemented with 100  $\mu\text{g/mL}$  SDS, 200  $\mu\text{g/mL}$  CFW, or 5 mM  $H_2O_2$  to assess plasma membrane, cell wall, and oxidative stress responses, respectively. (B) Quantification of growth inhibition rates under different stress conditions. Data are presented as the mean  $\pm$  SD from three independent biological replicates. Statistical significance was determined by one-way ANOVA. Differences were considered statistically significant at \*\*  $p < 0.01$  and \*\*\*  $p < 0.001$ .

### 3.6. Deletion of *adol*, *defl*, and *adk1* Affects Seed Infection-Related Pathogenicity in *A. flavus*

To further assess the contribution of *adol*, *defl*, and *adk1* to infection-related pathogenicity in *A. flavus*, peanut and maize seed infection assays were performed. In peanut infection assays, the three deletion mutants ( $\Delta adol$ ,  $\Delta defl$ , and  $\Delta adk1$ ) showed visibly reduced colonization compared with the WT strain, as indicated by weaker mycelial growth and reduced sporulation on the seed surface (Figure 6A). Quantification further confirmed that all three mutants produced markedly fewer spores on infected peanut seeds than the WT strain (Figure 6B). TLC analysis showed reduced AFB<sub>1</sub> accumulation in the  $\Delta adol$  and  $\Delta adk1$  mutants during peanut infection (Figure 6C,E,F), whereas the  $\Delta defl$  mutant produced AFB<sub>1</sub> at levels comparable to those of the WT strain (Figure 6C,D). A similar reduction in host colonization was observed in maize infection assays. Compared with the WT strain, the  $\Delta adol$ ,  $\Delta defl$ , and  $\Delta adk1$  mutants displayed weaker fungal growth and sporulation on maize kernels (Figure 6G), accompanied by markedly reduced spore production (Figure 6H). TLC analysis further showed that AFB<sub>1</sub> accumulation was reduced in the  $\Delta adol$  and  $\Delta adk1$  mutants (Figure 6 I,K,L), whereas the  $\Delta defl$  mutant accumulated higher levels of AFB<sub>1</sub> than the WT strain during maize infection (Figure 6I,J). These results suggest that deletion of *adol*, *defl*, or *adk1* impairs seed colonization and sporulation by *A. flavus*, whereas their effects on AFB<sub>1</sub> accumulation vary depending on the deleted gene and host substrate.

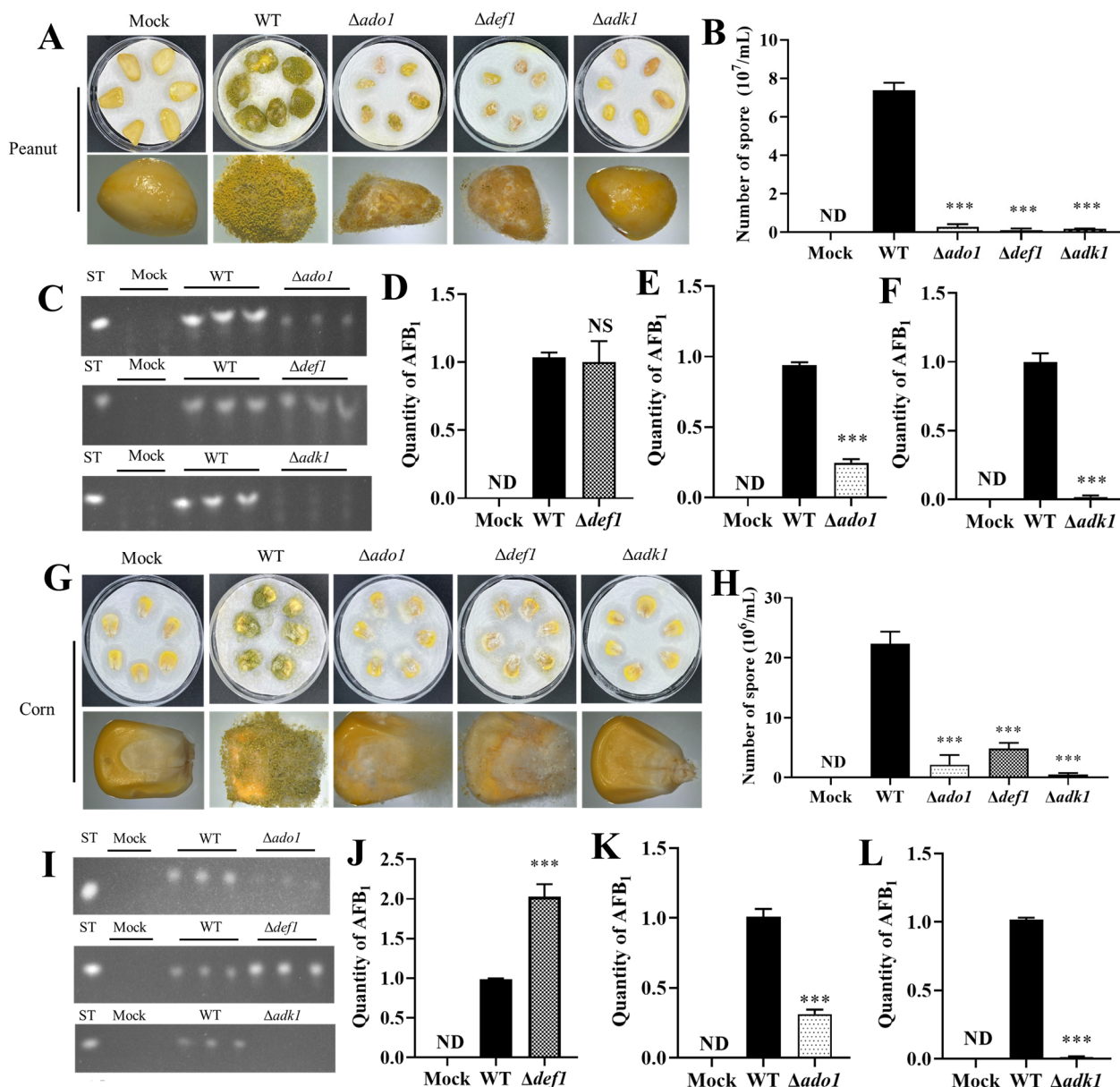


**Figure 6.** Effects of *ado1*, *def1*, and *adk1* deletion on pathogenicity in *A. flavus*. (A) Representative images of peanut seeds infected with the WT strain and  $\Delta ado1$ ,  $\Delta def1$ , and  $\Delta adk1$  mutants. (B) Quantification of conidia produced on infected peanut seeds. (C) TLC analysis of aflatoxin production in infected peanut seeds. (D–F) Quantitative analysis of aflatoxin production by  $\Delta ado1$ ,  $\Delta def1$ , and  $\Delta adk1$  on peanut seeds relative to the WT strain. (G) Representative images of maize seeds infected with the WT strain and mutant strains. (H) Quantification of conidia produced on infected maize seeds. (I) TLC analysis of aflatoxin production in infected maize seeds. (J–L) Quantitative analysis of aflatoxin production by  $\Delta ado1$ ,  $\Delta def1$ , and  $\Delta adk1$  on maize seeds relative to the wild-type strain. Data are presented as the mean  $\pm$  SD from three independent biological replicates. Statistical significance was determined by one-way ANOVA. Differences were considered statistically significant as \*\*\*  $p < 0.001$ .

#### 4. Discussion

Here, we characterized the interaction between AnAFP and *A. flavus*. We established a recombinant expression and purification strategy that yielded soluble AnAFP with inhibitory activity against *A. flavus*. We further investigated the contribution of *ado1*, *def1*, and *adk1* to AFP susceptibility and fungal developmental processes in *A. flavus*. Our findings suggest that AnAFP has potential as an antifungal protein against *A. flavus* and that *ado1*, *def1*, and *adk1* contribute to AFP tolerance, fungal development, stress responses, and aflatoxin production.

Cysteine-stabilized AFPs, particularly those produced by *Eurotiales* fungi, have attracted considerable interest as potential antifungal agents because of their small size and potent antifungal activity [39,40]. However, the heterologous production of cysteine-rich AFPs remains technically challenging. Unlike well-established yeast expression systems, filamentous fungi naturally form mycelial structures during cultivation, which makes large-scale and standardized protein production less convenient. In *A. niger*, AnAFP expression is closely associated with carbon starvation, nutrient recycling, and autophagy [41,42]. Previous studies have also reported a temporal disconnect between the accumulation of ANAFP transcripts and the extracellular detection of AnAFP [41,42]. In prokaryotic systems such as *E. coli*, inefficient disulfide-bond formation, protein misfolding, and inclusion body formation can further limit the yield of soluble and functional AFPs [12,43,44]. These factors highlight the difficulty of achieving reliable production of functional AFPs using native or conventional expression systems. To overcome these challenges, we established an *E. coli*-based expression strategy adapted to the predicted structural features of AnAFP. Similar expression strategies had previously been applied to PgAFP and AfAFP [13], prompting us to test whether this approach could also support the soluble production of AnAFP. Instead of expressing the full-length precursor, we focused on the predicted mature region of AnAFP, excluding the signal peptide, putative propeptide, and intrinsically disordered N-terminal segment. Although the removed N-terminal residues may contribute to secretion, processing, folding efficiency, or stability in the native fungal host, they are not predicted to constitute the mature cysteine-rich antifungal domain. The retained antifungal activity of recombinant AnAFP indicates that the predicted mature region is sufficient to inhibit *A. flavus*. This strategy enabled soluble expression and subsequent purification of recombinant AnAFP, providing a practical basis for evaluating its antifungal activity against *A. flavus*.

Mutant analysis showed that deletion of *adol*, *defl*, or *adk1* was associated with increased susceptibility of *A. flavus* to AnAFP, suggesting that these genes may contribute to AFP tolerance. *adk1* encodes adenylate kinase, an enzyme involved in the interconversion of adenine nucleotides and the maintenance of cellular energy balance [45,46]. *adol* encodes adenosine kinase, which phosphorylates adenosine and participates in the recycling of adenosine generated through the methyl cycle [23,47]. Considering these previous findings together with our results, we speculate that the increased AnAFP sensitivity of the  $\Delta adol$  and  $\Delta adk1$  mutants may be related to a reduced ability to adjust nucleotide and energy metabolism under AFP-induced stress. Because *adk1* is involved in adenine nucleotide homeostasis and ATP metabolism, deletion of *adk1* may reduce the capacity of *A. flavus* to buffer AnAFP-induced stress. The induction of *laeA* after AnAFP treatment in the  $\Delta adk1$  mutant may therefore represent stress-associated transcriptional rewiring rather than a simple restoration of the basal developmental programme. However, further biochemical and metabolic analyses will be required to test this possibility directly. In contrast, *defl* may contribute to AnAFP tolerance through a different process, possibly related to transcriptional stress management. In contrast, *defl* may contribute to AnAFP tolerance through a different process, possibly related to transcriptional stress management [24,48]. AFPs are known to impose cell-wall and membrane-associated stress in susceptible fungi, including inhibition of chitin synthesis, perturbation of membrane integrity, and activation of the cell-wall integrity pathway [14,18,49]. Therefore, rapid transcriptional adjustment may be important for fungal adaptation during AFP exposure. In this context, deletion of *defl* could potentially impair the ability of *A. flavus* to coordinate stress-responsive transcriptional responses upon AnAFP treatment. Collectively, these findings suggest that the increased AnAFP sensitivity of  $\Delta adol$ ,  $\Delta adk1$ , and  $\Delta defl$  may not result from disruption of a single resistance pathway. The current results should be interpreted as preliminary evidence that *adol*, *defl*, and *adk1* are associated with AFP sensitivity, fungal development, stress responses, aflatoxin production, and infection-related phenotypes in *A. flavus*. Future studies involving complemented strains, metabolic profiling, and transcriptome-wide analyses will be necessary to establish gene-specific causality and define the mechanisms by which these genes contribute to AFP tolerance and fungal physiology.

*laeA*, *veA*, and *wetA* are important regulatory genes associated with development, sporulation, stress responses, and secondary metabolism in *A. flavus* [38,50,51]. The *velB-veA-laeA* complex has been proposed to link developmental programmes with secondary metabolic output, and *laeA* is widely regarded as a global regulator of secondary metabolite gene clusters [52–55]. In *A. flavus*, *veA* and *laeA* have been reported to contribute to aflatoxin biosynthesis, sclerotial formation, and seed colonization [56]. By contrast, *wetA* is a multifunctional regulator that couples conidial maturation and survival with stress tolerance and chemical development in *A. flavus* [38]. In our study, AnAFP treatment induced different expression patterns of *laeA*, *veA*, and *wetA* in the WT strain and deletion mutants. These mutant transcriptional changes suggest that deletion of *ado1*, *def1*, or *adk1* may alter the transcriptional response of *A. flavus* to AnAFP. Thus, the altered expression of *laeA*, *veA*, and *wetA* may represent an indirect consequence of broader changes in developmental and secondary metabolism-related regulatory networks upon AnAFP exposure. We acknowledge that the RT-qPCR analysis in this study was limited to selected developmental and secondary metabolism-related regulators. Although SDS, CFW, and H<sub>2</sub>O<sub>2</sub> assays provided phenotypic evidence that deletion of *ado1*, *def1*, and *adk1* alters stress responses, additional transcriptional analysis of cell wall-, membrane-, and oxidative stress-related genes will be needed to define the stress-response pathways involved in AFP tolerance more comprehensively.

### Supplementary Materials

The following supporting information can be found at: <https://www.sciepublish.com/article/pii/1091>, Table S1: The quantitative reverse transcription-polymerase chain reaction primers used in this study.

### Author Contributions

Conceptualization, Z.L. and Y.W.; Methodology, Y.W.; Software, Z.L., S.W. (Sen Wang) and X.H.; Validation, J.S., Z.L. and S.W. (Sen Wang); Formal Analysis, Y.W.; Investigation, S.W. (Shihua Wang); Resources, Y.W.; Data Curation, Z.L.; Writing—Original Draft Preparation, Z.L.; Writing—Review & Editing, Y.W. and S.W. (Shihua Wang); Visualization, Z.L., S.W. (Sen Wang), Y.W. and J.S.; Supervision, S.W. (Shihua Wang); Project Administration, S.W. (Shihua Wang); Funding Acquisition, S.W. (Shihua Wang).

### Ethics Statement

Not applicable.

### Informed Consent Statement

Not applicable.

### Data Availability Statement

The authors confirm that the data supporting the findings of this study are available within the article.

### Funding

This work was supported by the National Natural Science Foundation of China (Grant No. 32370205), the Natural Science Foundation of Fujian Province (Grant No. 2026J001289) and the Science and Technology Innovation Project of Fujian Agriculture and Forestry University (Grant No. 463 KFB23082A).

### Declaration of Competing Interest

The authors declare that they have no known competing financial interests or personal relationships that could have appeared to influence the work reported in this paper.

## References

1. Mamo FT, Abate BA, Zheng Y, Nie C, He M, Liu Y. Distribution of *Aspergillus* Fungi and Recent Aflatoxin Reports, Health Risks, and Advances in Developments of Biological Mitigation Strategies in China. *Toxins* **2021**, *13*, 678. DOI:10.3390/toxins13100678
2. Amaike S, Keller NP. *Aspergillus flavus*. *Annu. Rev. Phytopathol.* **2011**, *49*, 107–133. DOI:10.1146/annurev-phyto-072910-095221
3. Salehi M, Khajavirad N, Seifi A, Salahshour F, Jahanbin B, Kazemizadeh H, et al. Proven *Aspergillus flavus* pulmonary aspergillosis in a COVID-19 patient: A case report and review of the literature. *Mycoses* **2021**, *64*, 809–816. DOI:10.1111/myc.13255
4. Liu Y, Wu F. Global Burden of Aflatoxin-Induced Hepatocellular Carcinoma: A Risk Assessment. *Environ. Health Perspect.* **2010**, *118*, 818–824. DOI:10.1289/ehp.0901388
5. Djenontin E, Lavergne R, Morio F, Dannaoui E. Antifungal Resistance in Non-*fumigatus* *Aspergillus* Species. *Mycoses* **2025**, *68*. DOI:10.1111/myc.70051
6. Huber A, Hajdu D, Bratschun-Khan D, Gaspari Z, Varbanov M, Philippot S, et al. New Antimicrobial Potential and Structural Properties of PAFB: A Cationic, Cysteine-Rich Protein from *Penicillium chrysogenum* Q176. *Sci. Rep.* **2018**, *8*, 1751. DOI:10.1038/s41598-018-20002-2
7. Garrigues S, Gandía M, Marcos JF. Occurrence and function of fungal antifungal proteins: a case study of the citrus postharvest pathogen *Penicillium digitatum*. *Appl. Microbiol. Biotechnol.* **2015**, *100*, 2243–2256. DOI:10.1007/s00253-015-7110-3
8. Mahlapuu M, Håkansson J, Ringstad L, Björn C. Antimicrobial Peptides: An Emerging Category of Therapeutic Agents. *Front. Cell. Infect. Microbiol.* **2016**, *6*, 194. DOI:10.3389/fcimb.2016.00194
9. Dehghan P, Bui T, Campbell LT, Lai YW, Tran-Dinh N, Zaini F, et al. Multilocus variable-number tandem-repeat analysis of clinical isolates of *Aspergillus flavus* from Iran reveals the first cases of *Aspergillus minisclerotigenes* associated with human infection. *BMC Infect. Dis.* **2014**, *14*, 358. DOI:10.1186/1471-2334-14-358
10. Bugeđa A, Shi X, Castillo L, Marcos JF, Manzanares P, López-Moya JJ, et al. High yield production of the antifungal proteins PeAfpA and PdAfpB by vacuole targeting in a TMV-based expression vector. *Plant Biotechnol. J.* **2025**, *24*, 313–327. DOI:10.1111/pbi.70093
11. Kharrat O, Yamaryo-Botté Y, Nasreddine R, Voisin S, Aumer T, Cammue BPA, et al. The antimicrobial activity of ETD151 defensin is dictated by the presence of glycosphingolipids in the targeted organisms. *Proc. Natl. Acad. Sci. USA* **2025**, *122*, e2415524122. DOI:10.1073/pnas.2415524122
12. Chen YP, Li Y, Chen F, Wu H, Zhang S. Characterization and expression of fungal defensin in *Escherichia coli* and its antifungal mechanism by RNA-seq analysis. *Front. Microbiol.* **2023**, *14*, 172257. DOI:10.3389/fmicb.2023.1172257
13. Wang Y, Wang S, Chen Y, Xie C, Xu H, Lin Y, et al. The role of Npt1 in regulating antifungal protein activity in filamentous fungi. *Nat. Commun.* **2025**, *16*, 2850. DOI:10.1038/s41467-025-58230-6
14. Hagen S, Marx F, Ram AF, Meyer V. The Antifungal Protein AFP from *Aspergillus giganteus* Inhibits Chitin Synthesis in Sensitive Fungi. *Appl. Environ. Microbiol.* **2007**, *73*, 2128–2134. DOI:10.1128/aem.02497-06
15. Wu Y, Zhang M, Yang Y, Ding X, Yang P, Huang K, et al. Structures and mechanism of chitin synthase and its inhibition by antifungal drug Nikkomycin Z. *Cell Discov.* **2022**, *8*, 129. DOI:10.1038/s41421-022-00495-y
16. Ren Z, Chhetri A, Guan Z, Suo Y, Yokoyama K, Lee SY. Structural basis for inhibition and regulation of a chitin synthase from *Candida albicans*. *Nat. Struct. Mol. Biol.* **2022**, *29*, 653–664. DOI:10.1038/s41594-022-00791-x
17. Gow NAR, Lenardon MD. Architecture of the dynamic fungal cell wall. *Nat. Rev. Microbiol.* **2022**, *21*, 248–259. DOI:10.1038/s41579-022-00796-9
18. Leiter E, Szappanos H, Oberparleiter C, Kaiserer L, Csernoch L, Pusztahelyi T, et al. Antifungal Protein PAF Severely Affects the Integrity of the Plasma Membrane of *Aspergillus nidulans* and Induces an Apoptosis-Like Phenotype. *Antimicrob. Agents Chemother.* **2005**, *49*, 2445–2453. DOI:10.1128/aac.49.6.2445-2453.2005
19. Binder U, Oberparleiter C, Meyer V, Marx F. The antifungal protein PAF interferes with PKC/MPK and cAMP/PKA signalling of *Aspergillus nidulans*. *Mol. Microbiol.* **2010**, *75*, 294–307. DOI:10.1111/j.1365-2958.2009.06936.x
20. Gun Lee D, Shin SY, Maeng CY, Jin ZZ, Kim KL, Hahm KS. Isolation and characterization of a novel antifungal peptide from *Aspergillus niger*. *Biochem. Biophys. Res. Commun.* **1999**, *263*, 646–651. DOI:10.1006/bbrc.1999.1428
21. Pel HJ, de Winde JH, Archer DB, Dyer PS, Hofmann G, Schaap PJ, et al. Genome sequencing and analysis of the versatile cell factory *Aspergillus niger* CBS 513.88. *Nat. Biotechnol.* **2007**, *25*, 221–231. DOI:10.1038/nbt1282

22. Aerts AM, Bammens L, Govaert G, Carmona-Gutierrez D, Madeo F, Cammue BPA, et al. The Antifungal Plant Defensin HsAFP1 from *Heuchera Sanguinea* Induces Apoptosis in *Candida Albicans*. *Front. Microbiol.* **2011**, *2*, 47. DOI:10.3389/fmicb.2011.00047
23. Kanai M, Masuda M, Takaoka Y, Ikeda H, Masaki K, Fujii T, et al. Adenosine kinase-deficient mutant of *Saccharomyces cerevisiae* accumulates S-adenosylmethionine because of an enhanced methionine biosynthesis pathway. *Appl. Microbiol. Biotechnol.* **2012**, *97*, 1183–1190. DOI:10.1007/s00253-012-4261-3
24. Woudstra EC, Gilbert C, Fellows J, Jansen L, Brouwer J, Erdjument-Bromage H, et al. A Rad26–Def1 complex coordinates repair and RNA pol II proteolysis in response to DNA damage. *Nature* **2002**, *415*, 929–933. DOI:10.1038/415929a
25. Chang PK, Scharfenstein LL, Wei Q, Bhatnagar D. Development and refinement of a high-efficiency gene-targeting system for *Aspergillus flavus*. *J. Microbiol. Methods* **2010**, *81*, 240–246. DOI:10.1016/j.mimet.2010.03.010
26. Rao Q, Guo W, Chen X. Identification and Characterization of an Antifungal Protein, AfAFPR9, Produced by Marine-Derived *Aspergillus fumigatus* R9. *J. Microbiol. Biotechnol.* **2015**, *25*, 620–628. DOI:10.4014/jmb.1409.09071
27. Martínez-Culebras PV, Gandía M, Boronat A, Marcos JF, Manzanares P. Differential susceptibility of mycotoxin-producing fungi to distinct antifungal proteins (AFPs). *Food Microbiol.* **2021**, *97*, 103760. DOI:10.1016/j.fm.2021.103760
28. Nolan T, Hands RE, Bustin SA. Quantification of mRNA using real-time RT-PCR. *Nat. Protoc.* **2006**, *1*, 1559–1582. DOI:10.1038/nprot.2006.236
29. Zhang F, Xu G, Geng L, Lu X, Yang K, Yuan J, et al. The Stress Response Regulator AflSkn7 Influences Morphological Development, Stress Response, and Pathogenicity in the Fungus *Aspergillus flavus*. *Toxins* **2016**, *8*, 202. DOI:10.3390/toxins8070202
30. Yang G, Cao X, Qin L, Yan L, Hong R, Yuan J, et al. Ssu72 Regulates Fungal Development, Aflatoxin Biosynthesis and Pathogenicity in *Aspergillus flavus*. *Toxins* **2020**, *12*, 717. DOI:10.3390/toxins12110717
31. Li G, Cao X, Tumukunde E, Zeng Q, Wang S. The target of rapamycin signaling pathway regulates vegetative development, aflatoxin biosynthesis, and pathogenicity in *Aspergillus flavus*. *eLife* **2024**, *12*, RP89478. DOI:10.7554/eLife.89478
32. Yang G, Cao X, Ma G, Qin L, Wu Y, Lin J, et al. MAPK pathway-related tyrosine phosphatases regulate development, secondary metabolism and pathogenicity in fungus *Aspergillus flavus*. *Environ. Microbiol.* **2020**, *22*, 5232–5247. DOI:10.1111/1462-2920.15202
33. Huber A, Galgóczy L, Váradi G, Holzkecht J, Kakar A, Malanovic N, et al. Two small, cysteine-rich and cationic antifungal proteins from *Penicillium chrysogenum*: A comparative study of PAF and PAFB. *Biochim. Biophys. Acta (BBA) – Biomembr.* **2020**, *1862*, 183246. DOI:10.1016/j.bbmem.2020.183246
34. Sonderegger C, Váradi G, Galgóczy L, Kocsubé S, Posch W, Borics A, et al. The Evolutionary Conserved  $\gamma$ -Core Motif Influences the Anti-*Candida* Activity of the *Penicillium chrysogenum* Antifungal Protein PAF. *Front. Microbiol.* **2018**, *9*, 1655. DOI:10.3389/fmicb.2018.01655
35. Liu Y, Wang X, Liu B. A comprehensive review and comparison of existing computational methods for intrinsically disordered protein and region prediction. *Brief. Bioinf.* **2019**, *20*, 330–346. DOI:10.1093/bib/bbx126
36. Kale SP, Milde L, Trapp MK, Frisvad JC, Keller NP, Bok JW. Requirement of LaeA for secondary metabolism and sclerotial production in *Aspergillus flavus*. *Fungal Genet. Biol.* **2008**, *45*, 1422–1429. DOI:10.1016/j.fgb.2008.06.009
37. Duran RM, Cary JW, Calvo AM. Production of cyclopiazonic acid, aflatrem, and aflatoxin by *Aspergillus flavus* is regulated by veA, a gene necessary for sclerotial formation. *Appl. Microbiol. Biotechnol.* **2007**, *73*, 1158–1168. DOI:10.1007/s00253-006-0581-5
38. Wu MY, Mead ME, Kim SC, Rokas A, Yu JH, Harris S. WetA bridges cellular and chemical development in *Aspergillus flavus*. *PLoS ONE* **2017**, *12*, e0179571. DOI:10.1371/journal.pone.0179571
39. Holzkecht J, Marx F. Navigating the fungal battlefield: cysteine-rich antifungal proteins and peptides from Eurotiales. *Front. Fungal Biol.* **2024**, *5*, 1451455. DOI:10.3389/ffunb.2024.1451455
40. Garrigues S, Gandía M, Popa C, Borics A, Marx F, Coca M, et al. Efficient production and characterization of the novel and highly active antifungal protein AfpB from *Penicillium digitatum*. *Sci. Rep.* **2017**, *7*, 14663. DOI:10.1038/s41598-017-15277-w
41. Paegle N, Jung S, Schäpe P, Müller-Hagen D, Ouedraogo JP, Heiderich C, et al. A Transcriptome Meta-Analysis Proposes Novel Biological Roles for the Antifungal Protein AnAFP in *Aspergillus niger*. *PLoS ONE* **2016**, *11*, e0165755. DOI:10.1371/journal.pone.0165755
42. Starke S, Velleman L, Dobbert B, Seibert L, Witte J, Jung S, et al. The antifungal peptide AnAFP from *Aspergillus niger* promotes nutrient mobilization through autophagic recycling during asexual development. *Front. Microbiol.* **2025**, *15*, 1490293. DOI:10.3389/fmicb.2024.1490293
43. Costa S, Almeida A, Castro A, Domingues L. Fusion tags for protein solubility, purification and immunogenicity in *Escherichia coli*: the novel Fh8 system. *Front. Microbiol.* **2014**, *5*, 63. DOI:10.3389/fmicb.2014.00063

44. Bhatwa A, Wang W, Hassan YI, Abraham N, Li XZ, Zhou T. Challenges Associated with the Formation of Recombinant Protein Inclusion Bodies in *Escherichia coli* and Strategies to Address Them for Industrial Applications. *Front. Bioeng. Biotechnol.* **2021**, *9*, 630551. DOI:10.3389/fbioe.2021.630551
45. Su X, Lu G, Li X, Rehman L, Liu W, Sun G, et al. Host-Induced Gene Silencing of an Adenylate Kinase Gene Involved in Fungal Energy Metabolism Improves Plant Resistance to *Verticillium dahliae*. *Biomolecules* **2020**, *10*, 127. DOI:10.3390/biom10010127
46. Dzeja P, Terzic A. Adenylate Kinase and AMP Signaling Networks: Metabolic Monitoring, Signal Communication and Body Energy Sensing. *IJMS* **2009**, *10*, 1729–1772. DOI:10.3390/ijms10041729
47. Lecoq K, Belloc I, Desgranges C, Daignan-Fornier B. Role of adenosine kinase in *Saccharomyces cerevisiae*: identification of the ADO1 gene and study of the mutant phenotypes. *Yeast* **2001**, *18*, 335–342. DOI:10.1002/1097-0061(20010315)18:4<335::Aid-yea674>3.0.Co;2-x
48. Akinniyi OT, Reese JC. DEF1: Much more than an RNA polymerase degradation factor. *DNA Repair* **2021**, *107*, 103202. DOI:10.1016/j.dnarep.2021.103202
49. Ouedraogo JP, Hagen S, Spielvogel A, Engelhardt S, Meyer V. Survival Strategies of Yeast and Filamentous Fungi against the Antifungal Protein AFP. *J. Biol. Chem.* **2011**, *286*, 13859–13868. DOI:10.1074/jbc.M110.203588
50. Bayram O, Krappmann S, Ni M, Bok JW, Helmstaedt K, Valerius O, et al. VelB/VeA/LaeA Complex Coordinates Light Signal with Fungal Development and Secondary Metabolism. *Science* **2008**, *320*, 1504–1506. DOI:10.1126/science.1155888
51. Bok JW, Keller NP. LaeA, a Regulator of Secondary Metabolism in *Aspergillus* spp. *Eukaryot Cell* **2004**, *3*, 527–535. DOI:10.1128/ec.3.2.527-535.2004
52. Sarikaya Bayram Ö, Bayram Ö, Valerius O, Park HS, Irniger S, Gerke J, et al. LaeA Control of Velvet Family Regulatory Proteins for Light-Dependent Development and Fungal Cell-Type Specificity. *PLoS Genet.* **2010**, *6*, e1001226. DOI:10.1371/journal.pgen.1001226
53. Moon H, Lee MK, Bok I, Bok JW, Keller NP, Yu JH, et al. Unraveling the Gene Regulatory Networks of the Global Regulators VeA and LaeA in *Aspergillus nidulans*. *Microbiol. Spectr.* **2023**, *11*, e00166-23. DOI:10.1128/spectrum.00166-23
54. Perrin RM, Fedorova ND, Bok JW, Cramer RA, Wortman JR, Kim HS, et al. Transcriptional Regulation of Chemical Diversity in *Aspergillus fumigatus* by LaeA. *PLoS Pathog.* **2007**, *3*, e50. DOI:10.1371/journal.ppat.0030050
55. Palmer JM, Theisen JM, Duran RM, Grayburn WS, Calvo AM, Keller NP, et al. Secondary Metabolism and Development Is Mediated by LlmF Control of VeA Subcellular Localization in *Aspergillus nidulans*. *PLoS Genet.* **2013**, *9*, e1003193. DOI:10.1371/journal.pgen.1003193
56. Amaike S, Keller NP. Distinct Roles for VeA and LaeA in Development and Pathogenesis of *Aspergillus flavus*. *Eukaryot Cell* **2009**, *8*, 1051–1060. DOI:10.1128/ec.00088-09